IOP Conf. Series: Materials Science and Engineering **143** (2016) 012027 doi:10.1088/1757-899X/143/1/012027

Numeric simulations of a liquid metal model of a bloom caster under the effect of rotary electromagnetic stirring

M. Barna[1], M. Javurek[1], B. Willers[2], S. Eckert[2] and J. Reiter[3]

[1] Johannes Kepler University (JKU) Linz, Altenbergerstraße 69, 4040 Linz, Austria

[2] Helmholtz-Zentrum Dresden-Rossendorf (HZDR), P.O. Box 510119, 01314 Dresden, Germany

[3] voestalpine Stahl Donawitz GmbH, Kerpelystraße 199, 8700 Leoben, Austria

martin.barna@jku.at

Abstract. At the voestalpine Stahl Donawitz GmbH the continuous casting of round steel blooms is commonly supported by electromagnetically induced stirring of the liquid steel flow. A number of beneficial effects are attributed to electromagnetic stirring in the mould region (M-EMS), e.g. the enhanced transition from columnar to equiaxed solidification, the homogenization of the liquid steel flow or the reduction of surface and subsurface defects. Although the positive effects of M-EMS can be seen on the blooms (e.g. in etchings), the link between electromagnetic stirring of the steel melt and the quality of the solidified bloom is not sufficiently understood. Theoretical considerations are often limited to general cases and their results are therefore not directly applicable to real continuous casting geometries. On the other hand, plant measurements can only be performed to a limited extent due to the harsh conditions and other restrictions (e.g. safety regulations). In this work an alternative approach is used to investigate the steel flow in a round bloom caster under the influence of M-EMS. In a 1:3 scale Perspex model of a round bloom strand, measurements of the flow under the influence of a rotating magnetic field can be conducted. These measurements provide a validation benchmark for the numeric simulations. A numeric model of the before mentioned 1:3 scale model is implemented, encompassing the strand, the submerged entry nozzle as well as the M-EMS device. In the modelling approach, the bidirectional coupling between liquid steel flow and the electromagnetic field/forces has to be considered because otherwise the resulting tangential velocities will be overestimated. With the validated modelling approach, simulations of real casting machines can then be conducted, stirring parameter influences can be shown and conclusions for the real casting process can be drawn.

Introduction

In the continuous steel casting, electromagnetic stirring for (round) bloom casting is a quite widespread technique. It shall help to increase the productivity while maintaining/enhancing the quality of the product. Electromagnetic stirrers are used at various positions along the strand, with mould-electromagnetic stirrers (M-EMS) being the most established ones. These stirrers produce a magnetic field, which is nearly homogeneous over the cross section of the strand and rotates with a given frequency. Lorentz forces are induced, which excite a rotary motion in the liquid core of the strand. This imposed azimuthal flow of the liquid steel provides numerous benefits. Most important

for the product quality are the enhanced transition from globular to equiaxed solidification, the reduction of surface and subsurface defects and the homogenization of the liquid steel's temperature and composition. For the steel production, a correlation between the stirring parameters and a quality index (e.g. the percentage of equiaxed zone) is crucial to ensure a good product quality. These correlations can be found by employing plant measurements, experiments and/or numerical simulations

In this work the continuous casting of round blooms with mould-electromagnetic stirring is investigated primarily through numerical simulations validated by measurements made at a 1:3 strand model. A description of the experimental built-up and the considerations behind it are also included, while a detailed description of the experiment can be found in the paper of Willers et al. [1].

Mathematical and numerical modelling

The liquid steel flow inside the cast strand is governed by the Navier-Stokes equations. The high velocities of the liquid steel exiting the straight-through submerged entry nozzle (SEN) lead to a turbulent flow in the core, which is mathematically described by the Reynolds averaged Navier-Stokes equations (RANS), using the realizable k-ε model [2] for closure. The validation cases are simulated with the eutectic alloy $Ga_{68}In_{20}Sn_{12}$, which is treated as a Newtonian, incompressible and isothermal fluid. In the strand geometry, no symmetry is used in order to allow for asymmetric flow fluctuations. The strand walls and the mould level are modelled as rigid walls with the no-slip condition.

If electromagnetic fields are employed to modify the liquid steel flow, Maxwell's equations and Ohm's law are used to describe the magnetic field and its interaction with the liquid steel flow. Either a formulation for the magnetic vector potential A or the magnetic flux density B is used. The interaction between the liquid steel flow and the electromagnetic field is given on one hand by the velocity field and on the other hand by the electromagnetic Lorentz forces. So in general, a bi-directional coupling is used to correctly capture the interaction. In the present case, an inverse problem utilizing the potential theory is solved for the magnetic field of the stirrer. The resulting field distribution can then be used for e.g. the Spitzer method [3], [4].

$$\overline{F_r} = -\frac{1}{8} B_0^2 \left(\omega - \frac{v_t}{r} \right)^2 \sigma^2 \mu_M r^3$$
$$\overline{F_t} = \frac{1}{2} B_0^2 \left(\omega - \frac{v_t}{r} \right) \sigma r \qquad (1)$$

Equation 1 describes the radial and tangential force densities in dependence of the magnetic flux density B_0, the angular frequency of the magnetic field ω, the radial position r and the fluid's tangential velocity v_t. Also the material parameter, the electrical conductivity σ and the magnetic permeability μ_M, are needed. Alternatively, instead of using the solution of the inverse problem to directly compute the forces, it can be used in ANSYS Emag as a boundary condition on a spatially reduced electromagnetic model, which only encompasses the strand.

Physical modelling

A 1:3 scale model of the round bloom caster at voestalpine Stahl Donawitz GmbH (Figure 1) is built up at HZDR, made of acrylic glass. The model strand has an inner diameter of d=80 mm and a length of about L=800 mm. The inner diameter of the straight-through SEN is d_i=10 mm and its submersion depth is h_{SEN}=40 mm. The mould level is kept approximately 25 mm below the upper edge of the model strand. The strand curvature and the solidified shell are neglected.

The stirrer is located about 250 mm from the upper edge of the model strand, with an inner diameter of 200 mm and a height of 310 mm. The stirrer has a rather complex layout which makes it unfeasible for numerical simulation (Figure 2). So instead of building a model of the stirrer, an inverse problem, detailed below, is solved to approximate the magnetic field.

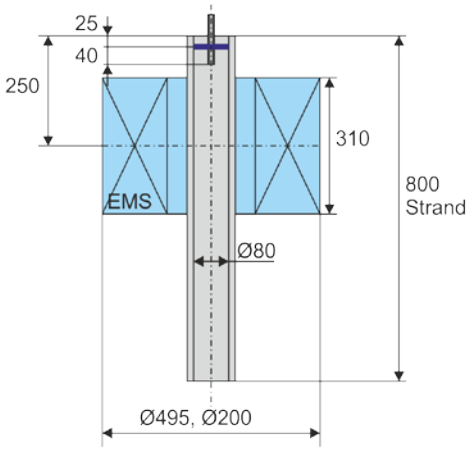

Figure 1: Draft of the 1:3 round bloom model with mould-electromagnetic stirring; grey: mould and SEN; blue: electromagnetic stirrer; the horizontal, purple line indicates the free surface

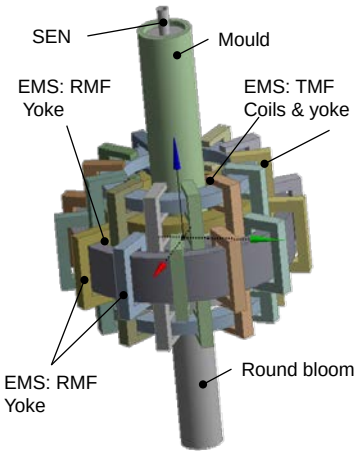

Figure 2: Layout of the electromagnetic stirrer from HZDR with mould, strand and submerged entry nozzle (SEN); RMF: rotating magnetic field, TMF: traveling magnetic field

For the validation, the time-averaged tangential velocities are measured at two distances from the stand axis, d=15 mm and d=30 mm. Additional details regarding the experimental setup, flow measurement and the UDV sensors and can be found in Willers et al. [1].

Results and Discussion

Dimensioning of the validation model:
In order to investigate the electromagnetic stirring for the continuous round bloom casting of steel, one must ensure that all phenomena, which are relevant for the real casting process, can be reproduced by the experiment. This can be easily achieved by consulting various dimensionless numbers. In the literature (e.g. [5]–[7]) two distinct numbers are used, the shielding parameter *S* (equation 4) and the interaction number *N* (also called Stuart number, equation 5).

$$S = \mu_M \sigma \omega R^2 = \frac{\text{diffusion time}}{\text{rotation period}} \tag{4}$$

$$N = \frac{\sigma B_0^2}{\rho \varpi} = \frac{\text{electromagnetic forces}}{\text{inertia forces}} \tag{5}$$

As the real casting slightly deviates from the above mentioned analytical case, additional parameters have to be considered. Turbulence plays an important role for the liquid steel flow of continuous casting. So the Taylor number *Ta*, which is the equivalent of the Reynolds number for rotating flows, is added to the spectrum of key figures.

$$\mathrm{Re}_{EMS} \propto Ta = \frac{\varpi^2 R^4}{\nu^2} = \frac{\text{inertia forces}}{\text{viscous forces}} \tag{6}$$

Electromagnetic stirring bears analogy to mechanical mixing/stirring, which is commonly used in various industries and extensively investigated. This knowledge was also used for dimensioning of the experiment and to ensure that it will properly represent the real continuous casting process. In Uhl and Gray [8] a figure can be found where the power number, essentially a flow drag coefficient, is plotted in dependence of the Reynolds number[1]. For values higher than $\mathrm{Re}_{EMS}>10^4$ the flow is turbulent and the power number is approximately constant. Depending on the geometry of the mechanic stirrer, this drag coefficient lies between 0.2 and 0.8.

[1] In mechanical mixing/stirring, the Reynolds number is usually build with the square of the mixer's diameter, the rotation speed in RPM and the viscosity of the fluid.

To characterize the flow induced by electromagnetic stirring, one can use this knowledge and equilibrate the electromagnetic power, imposed by the electromagnetic stirrer, with the drag of the fluid flow. The electromagnetic stirring power is given by equation 7. Here the force density formulation, derived by Spitzer [3], is used with the angular frequency of the fluid ω_{Fl}.

$$P_{mag} = \int_V \frac{1}{2} B_0^2(r,z)\left[\omega - \omega_{Fl}(r,z)\right]\sigma r^2 \omega_{Fl}(r,z)\,dV \tag{7}$$

For a first result, some simplifications have to be made: The magnitude of the magnetic flux density B_0 and the fluid rotational frequency ω_{Fl} are assumed to be independent of the radial and the axial coordinate, which will not be exactly true. In reality the stirrer has a finite length; hence an axial variation of both quantities will exist. Equation 7 can be simplified to

$$P_{mag} = \frac{1}{2}\overline{B_0}^2\left[\omega - \overline{\omega_{Fl}}\right]\overline{\omega_{Fl}}\sigma\frac{r^4}{4}\pi h\,, \tag{8}$$

where $h=C_{EMS}\cdot r$ represents the height of the stirrer and the quantities with the bar, $\overline{B_0}$, $\overline{\omega_{Fl}}$, are averaged values. The drag of the fluid flow is deduced from Uhl and Gray [8], by transforming the power number. As mentioned before, it is constant for $Re>10^4$

$$P_{drag} = \zeta_{Fl}\rho\overline{\omega_{Fl}}^3(2r)^5 \tag{9}$$

Equation 8 and 9 can now be put in equilibrium. The resulting polynomial equation of second order can be solved for the angular frequency of the fluid to estimate the average angular fluid flow, if the drag and stirring coefficient are known (see e.g. [9]). However, under the assumption that the fluid rotates on average at half the angular speed of the magnetic field, one can further simplify the equation to

$$\underbrace{\frac{1}{2^8}C_{EMS}\pi}_{\zeta_{mag}}\overline{B_0}^2\left[\omega - \overline{\omega_{Fl}}\right]\overline{\omega_{Fl}}\sigma r^5 = \zeta_{Fl}\rho\overline{\omega_{Fl}}^3 r^5\,. \tag{10}$$

In equation 10, the drag coefficient and the stirring coefficient are moved to the left side and the right side has the same structure as the interaction number N (equation 11). It is desirable that the experiment has the same ratio of electromagnetic forces to inertia forces as the real caster. This can be easily achieved with equation 13. For convenience the fluid's angular frequency of both setups shall be the same.

$$\frac{\zeta_{Fl}}{\zeta_{mag}} = \frac{\sigma\overline{B_0}^2}{\rho\overline{\omega_{Fl}}} = N_{calc} \rightarrow \text{const.} \tag{11}$$

$$\overline{B_{0,\text{experiment}}}^2 = \frac{\sigma_{\text{caster}}}{\sigma_{\text{experiment}}}\frac{\rho_{\text{experiment}}}{\rho_{\text{caster}}}\underbrace{\frac{\overline{\omega_{\text{Fl,experiment}}}}{\overline{\omega_{\text{Fl,caster}}}}}_{=1}\overline{B_{0,\text{caster}}}^2 \tag{13}$$

If the ratio of stirrer height to strand radius differs between experiment and real caster, it can also be considered in equation 13. This approximation can be used to correctly set the stirring parameters of the experiment similar to the real casting conditions.

Figure 3 depicts the range of all relevant key figures for experiment and real casting geometry next to each other. In addition, the critical values for the key figures are also presented in the figure (black horizontal lines). Arrows indicate whether it's favourable to stay above or below the critical value. It can be seen that the experiment covers much broader ranges than the real caster, which means that all important phenomena occurring at the caster are reproducible by the experiment. Only the range of the Reynolds number for the SEN is smaller in the experimental setup, but this should not pose a problem as the investigation is concentrated mainly on the electromagnetic stirring and less on the submerged

jet. For both setups the range of the shielding parameter *S* is near the critical value (of 1). So some distortion of the magnetic field may be observed, but the effect is accounted for in the numeric model.

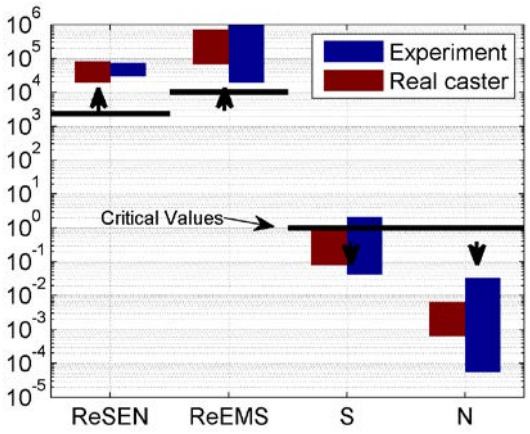

Figure 3: Graphical representation of the range of the key figures (Reynolds number of the SEN flow Re_{SEN} and the stirred flow Re_{EMS}, shielding parameter S and interaction number N) for the real caster (red) and the experiment (blue); critical values are designated by the black lines and arrows indicate the favourable region

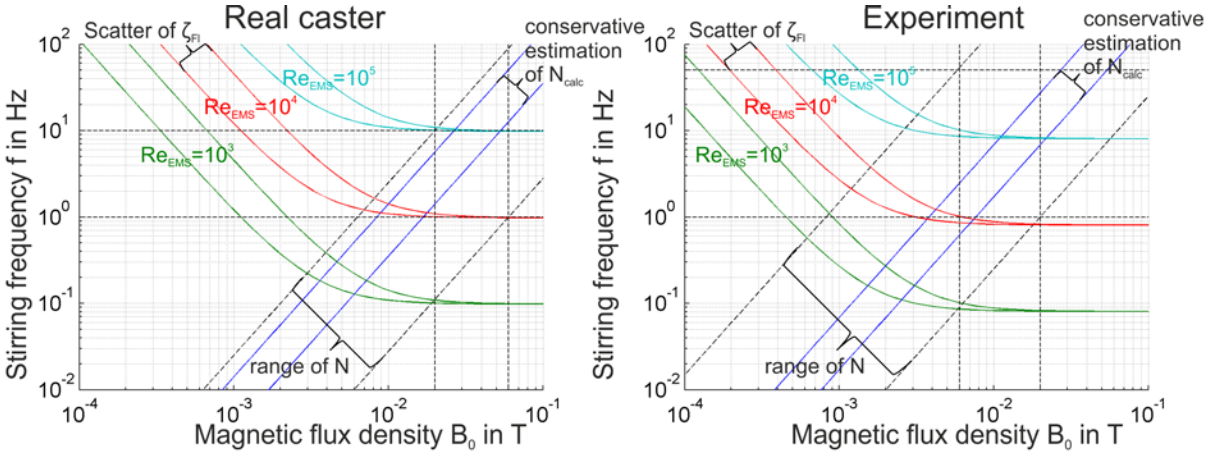

Figure 4: Range of magnetic flux density B_0 and stirring frequency f for the real caster and the experiment; interaction number N and Reynolds number Re_{EMS} for the strand are also plotted into the graph; due to the scatter of the drag coefficient (see [8]), there is some uncertainty in the Reynolds number; the blue lines show a conservative estimation of the calculated interaction number N_{calc} (equation 11) for both setups; as long as the Reynolds number is higher than 10^4 (turbulent regime) the flow regime in both operation windows will be similar and the experiment is able to represent the real casting situation.

The operating windows for the caster and the experiment are shown in Figure 4. The ranges of magnetic flux density and the stirring frequency give the limits of operation, which also provide the minimum and maximum of the interaction number. In addition, the Reynolds number of the rotating flow Re_{EMS} is plotted (with regard to the scattering of the drag coefficient, see [8]). Both cases, real caster and experiment, are operated in the turbulent flow regime (above $Re_{EMS}>10^4$) and within the operation limits. So the flow regime will be the same for the real caster and the experiment and the latter can correctly represent the flow in continuous steel casters with electromagnetic stirring.

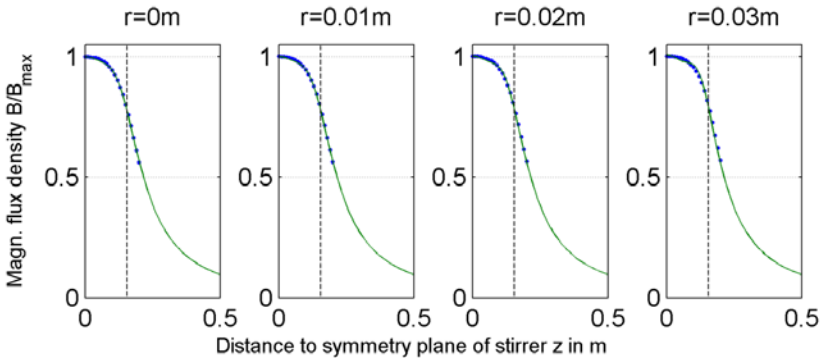

Figure 5: Comparison between measurements (blue dots) and approximation (green line) of electromagnetic stirring field for different radii plotted over the distance to the stirrer's middle plane, the black dashed line marks the edge of the stirrer

The electromagnetic field is approximated with the help of the potential theory. This guarantees that the solution will be solenoidal and without rotation, meaning per se no eddy currents will be induced. The complexity of the problem is reduced by assuming a radially and axially symmetric 2D arrangement of sinks and sources, which rotates around the strand with the stirring frequency. The resulting (magnetic) vector potential can then be employed either as a boundary condition for the electromagnetic solver or the magnetic flux density field can be calculated for the CFD model. Figure 5 compares the available measurements and the solution of the inverse problem. The curves show an overall good agreement, only at bigger radii ($r \geq 0.04$ m) outside the strand slight differences arise.

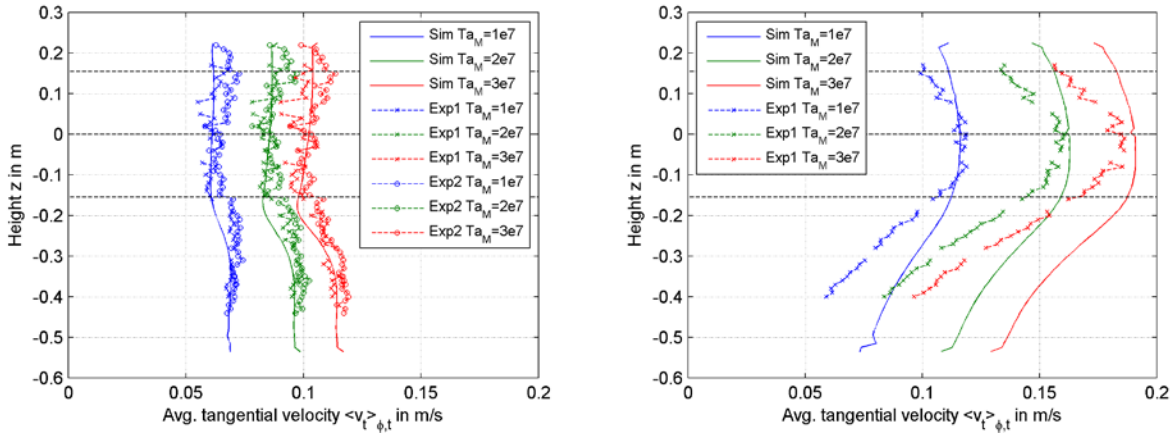

Figure 6: Average tangential velocity plotted over the height of the strand at d=15 mm (left) and d=30 mm (right) for the magnetic Taylor numbers Ta_M=1e7 (blue), Ta_M =2e7 (green) and Ta_M =3e7 (red); solid lines: simulation; markers (X, O) signify two separate measurements; horizontal lines mark the upper and lower edge of the stirrer as well as the symmetry plane

As stated before, analytical solutions exist for the electromagnetic stirring of an infinitely long cylinder (e.g. [3]–[6]) – even under the influence of axially non-uniform magnetic fields (e.g. [10], [11]). In real casters, contrasting to most analytical cases, the flow is turbulent and the stirring field often has a quite complex distribution. These facts make experimental and/or numerical approaches the more favorable means of investigation.

The first validation is done for three different values of the magnetic flux densities B_0={10.58; 14.96; 18.32} mT, which equal magnetic Taylor numbers Ta_M={1e7; 2e7; 3e7}[2]. For these three magnetic field strengths, cases solely with electromagnetic stirring are investigated. Afterwards the interaction of stirring with a mass flow through a SEN are investigated for Ta_M={1e7; 2e7}. The frequency of the

[2] The magnetic Taylor number is the ratio of the electromagnetic forces to the viscous forces.

stirrer is kept fixed at the stirring frequency used at the steel plant. The Spitzer method is used in conjunction with the approximation of the stirrer field for these validation cases.

Figure 6 depicts the average tangential velocity for a distance of d=15 mm and d=30 mm from the strand axis respectively for the simulation and the experiment. While the measurements are only averaged over time, the simulation results are in addition azimuthally averaged. For the distance d=30 mm the maximum tangential velocity is similar to the measurement results, but the tangential velocity decreases axially far slower (see Figure 6 right diagram). A possible reason could be an overestimation of the turbulent viscosity by the employed turbulence models. The left diagram in Figure 6 shows that, at the smaller distance d=15 mm, the measurements agree well with the simulation results. The increase of tangential velocity in the lower part can be correctly reproduced. The increase of the tangential velocity in the lower part of the strand is probably caused by the transport of angular momentum due to the secondary flow.

An axial offset between simulation results and measurements is observed in all investigated cases, those without and those with an imposed axial mass flow. A possible explanation is that the stirrer is not perfectly aligned inside its casing, which is used as reference for the positioning of strand and stirrer in the experiment.

Electromagnetic stirring and imposed axial mass flow:

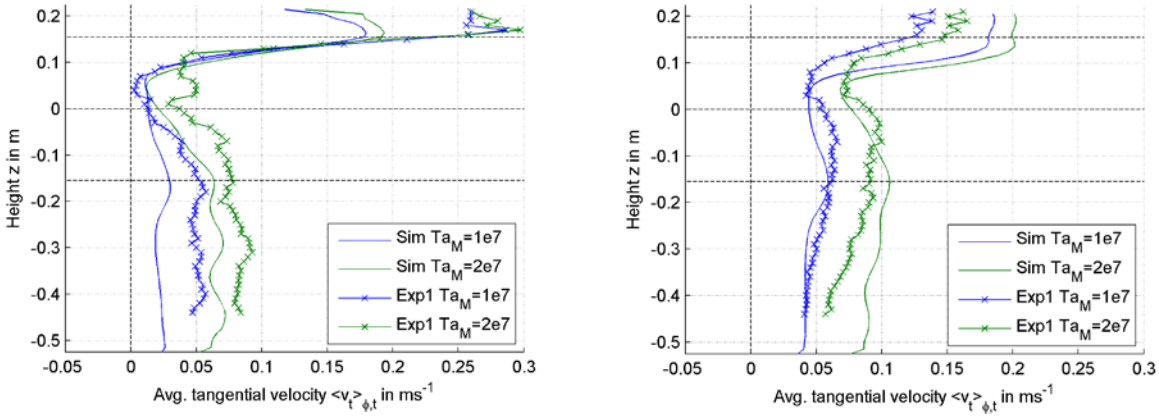

Figure 7: Average tangential velocity plotted over the height of the strand at d=15 mm (left) and d=30 mm (right) for the magnetic Taylor numbers Ta_M=1e7 (blue) and Ta_M=2e7 (green); inlet velocity v_{SEN} =1.3 ms^{-1}; solid lines: simulation; marker X: measurements; the horizontal lines mark the upper and lower edge of the stirrer as well as the symmetry plane

With the stirring validated, the next step is to investigate the influence of the submerged jet on to the flow in the strand. The velocity in the SEN is chosen to correspond to real casting situations (v_{SEN}=1.3 ms^{-1} equals a casting speed of ~1.0 mmin^{-1}). The frequency and stirring field strength of the electromagnetic stirring are kept fixed.

In the simulation a rigid plane wall is assumed, but in the experiment a thin, deformable oxide skin covers the free surface. Also in the vicinity of the SEN, a vortex (randomly) forms and rotates around the SEN. Both phenomena impact the velocity field in the vicinity of the free surface and through convection also the distribution of the tangential velocity further down the strand. Nonetheless, a comparison between the experimental and the numeric simulation is made. Qualitatively the results correspond well. Figure 7 depicts the measurements and simulation results at both radii. A good overall agreement is found (if the axial offset is compensated). But at the distance d=15 mm the simulation results underestimate the effect of the electromagnetic stirring and the transport of angular momentum from the mould region down into the strand (Figure 7 left diagram). The average tangential velocities for both cases are smaller than those in the measurements with the effect being more pronounced for the case Ta_M=1e7.

Conclusion

For the investigation of electromagnetic stirring in continuous casting of round blooms, a 1:3 scale model of the round strand and the mould-electromagnetic stirrer is designed. Analytical considerations show that this model is able to reproduce the flow in the round bloom caster of voestalpine Stahl Donawitz GmbH under the influence of the mould-stirrer quite well. An inverse problem is solved to approximate the magnetic stirring field.

Three different magnetic flux densities are investigated for sole electromagnetic stirring. The average tangential velocities are in good agreement for d=15 mm. For the distance d=30 mm, the simulations can capture the maximum quite well, but the measurements show a stronger axial decrease of the tangential velocity. Throughout the validation an axial offset between measurements and simulation could be observed. For the second part of the validation, an axial mass flow is added. The tangential velocity at d=30 mm is in overall good agreement. For the distance d=15 mm, the simulated tangential velocities are smaller than the measured ones. This deviation is attributed to the deformation of the free surface and a vortex at the SEN, which occurred (randomly) during the experiment and are not considered in the numeric model. The numeric model was validated with measurements and a detailed insight into an electromagnetically stirred flow could be gained. Based on this work, the numeric model can be used to further investigate electromagnetic stirring in continuous casting and investigate the impact of different parameter sets prior to real plant trials.

Acknowledgments

This work has been financially supported within the Austrian competence centre programme COMET by the BMVIT; by the BMWFJ; by the provinces of Upper Austria, Styria and Tyrol; by the SFG and by the Tiroler Zukunftsstiftung.

References

[1] B. Willers, M. Barna, J. Reiter, and S. Eckert, “Experimental investigation of electromagnetic stirring affecting the mould flow in a liquid metal model,” in *Proceedings of 2nd ESTAD 2015*, 2015.

[2] T.-H. Shih, W. W. Liou, A. Shabbir, Z. Yang, and J. Zhu, “A New k-e Eddy Viscosity Model for High Reynolds Number Turbulent Flows Model Development and Validation,” Cleveland, 1994.

[3] K.-H. Spitzer, “Berechnung von Strömungen beim elektromagnetischen Rotationsrühren von Rundsträngen,” Technische Universität Clausthal, 1985.

[4] K.-H. Spitzer, M. Dubke, and K. Schwerdtfeger, “Rotational Electromagnetic Stirring in Continuous Casting of Round Strands,” *Metall. Mater. Trans. B*, vol. 17, pp. 119–131, 1986.

[5] R. Moreau, *Magnetohydrodynamics*. Dordrecht: Kluwer Academic Publishers, 1990.

[6] A. Alemany and R. Moreau, “Ècoulement d’un fluide conducteur de l'électricité en présence d'un champ magnétique tournant,” *J. Mécanique*, vol. 16, no. 4, pp. 625–646, 1977.

[7] H. K. Moffatt, “On fluid flow induced by a rotating magnetic field,” *J. Fluid Mech.*, vol. 22, no. 3, pp. 521–528, 1965.

[8] V. Uhl and J. B. Gray, *Mixing – Theory and Practice*. New York, NY: Academic Press, 1966.

[9] M. Barna, “Untersuchungen der Flüssigstahlströmung beim Rundstranggießen mit elektromagnetischem Kokillenrührer,” Johannes Kepler Universität Linz, 2013.

[10] P. A. Davidson, “Analytical models of rotary electromagnetic stirring,” *IMA J. Manag. Math.*, vol. 7, no. 1, pp. 89–108, Jan. 1996.

[11] P. A. Davidson and J. C. R. Hunt, “Swirling recirculating flow an a liquid-metal column generated by a rotating magnetic field,” *J. Fluid Mech.*, vol. 185, pp. 67–106, Apr. 1987.